

Improving the Resistance of Molecularly Doped Polymer Semiconductor Layers to Solvent

Dominique Lungwitz, Ahmed E. Mansour, Yadong Zhang, Andreas Opitz, Stephen Barlow, Seth R. Marder, and Norbert Koch*



Cite This: *Chem. Mater.* 2023, 35, 672–681



Read Online

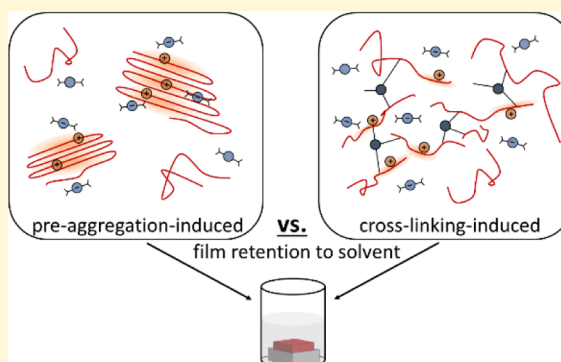
ACCESS |

Metrics & More

Article Recommendations

Supporting Information

ABSTRACT: The ability to form multi-heterolayer (opto)electronic devices by solution processing of (molecularly doped) semiconducting polymer layers is of great interest since it can facilitate the fabrication of large-area and low-cost devices. However, the solution processing of multilayer devices poses a particular challenge with regard to dissolution of the first layer during the deposition of a second layer. Several approaches have been introduced to circumvent this problem for neat polymers, but suitable approaches for molecularly doped polymer semiconductors are much less well-developed. Here, we provide insights into two different mechanisms that can enhance the solvent resistance of solution-processed doped polymer layers while also retaining the dopants, one being the doping-induced pre-aggregation in solution and the other including the use of a photo-reactive agent that results in covalent cross-linking of the semiconductor and, perhaps in some cases, the dopant. For molecularly p-doped poly(3-hexylthiophene-2,5-diyl) and poly[2,5-bis(3-tetradecyl-thiophene-2-yl)thieno(3,2-*b*)thiophene] layers, we find that the formation of polymer chain aggregates prior to the deposition from solution plays a major role in enhancing solvent resistance. However, this pre-aggregation limits inclusion of the cross-linking agent benzene-1,3,5-triyl tris(4-azido-2,3,5,6-tetrafluorobenzoate). We show that if pre-aggregation in solution is suppressed, high resistance of thin doped polymer layers to solvent can be achieved using the tris(azide). Moreover, the electrical conductivity can be largely retained by increasing the tris(azide) content in a doped polymer layer.



INTRODUCTION

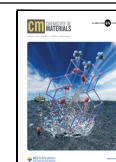
Organic electronic and optoelectronic devices typically feature multi-heterolayer structures, comprising different organic semiconductor layers, some of which may be doped, that can facilitate charge carrier injection, recombination, or dissociation at the interfaces between layers. Using solution processing to deposit organic semiconductor polymer layers on top of each other can enable large-area and low-cost fabrication of complex multilayer devices but is challenging. After the formation of the first layer, the solvent used for deposition of the second layer may redissolve the underlying first layer. This is particularly relevant for molecularly doped polymer layers since doping can enhance the performance of many devices such as organic light-emitting diodes, organic photovoltaic cells, and organic field-effect transistors.^{1–4} By admixing a few mole percent of a molecular dopant with an electron affinity (EA) that is roughly equal to, or larger than, the ionization energy (IE) of the semiconductor for p-type doping (or vice versa for n-type doping), the hole (electron) density can be increased, and the Fermi level position can be precisely controlled. Preventing dissolution of doped layers and selective removal of molecular dopants by contact with solvents is, therefore, essential.

One approach for the fabrication of multilayer solution-processed structures is the use of orthogonal solvents. Here, the solvent used to deposit a second layer on the top of a first layer is unable to dissolve the first layer.^{5–7} However, this technique suffers from limitations since many organic semiconductors possess similar solubility in common organic solvents so that it is generally challenging, and often not possible, to find a suitable solvent in which the second semiconductor is highly soluble and the first one essentially insoluble. Lamination of preformed layers has also been used in some cases, including between a p-doped polymer and a photovoltaic bulk heterojunction blend,⁸ although the use of water in this method limits its applicability, especially in the case of n-doped systems. The alternative approach of covalent cross-linking has been proven to be a versatile tool to form insoluble polymer layers, which can find application in

Received: October 27, 2022

Revised: December 20, 2022

Published: January 4, 2023



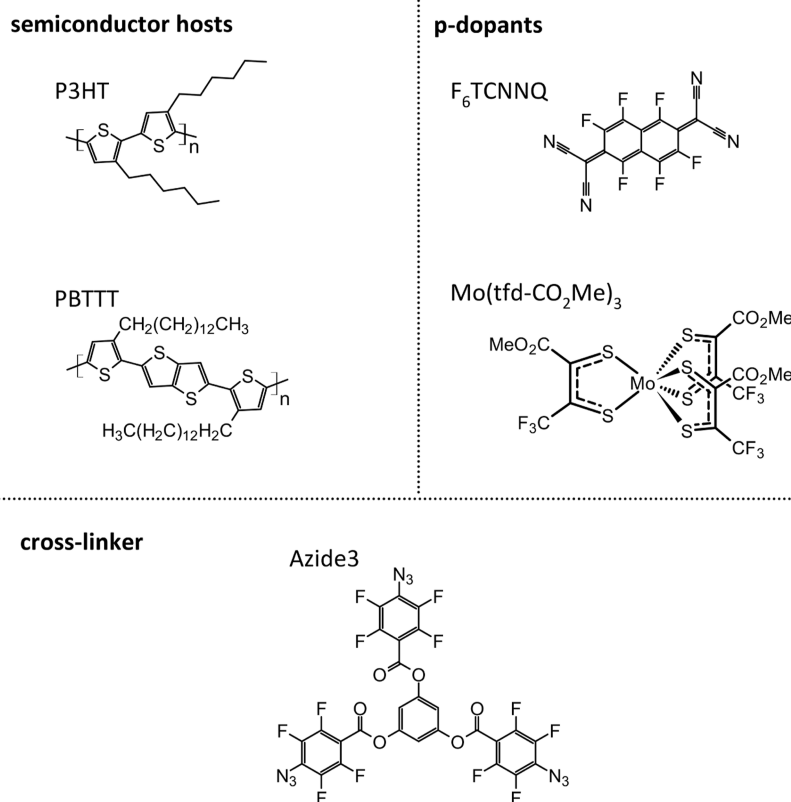


Figure 1. Chemical structures of the materials used in this study: P3HT, PBTTT, F₆TCNNQ, [Mo(tfd-CO₂Me)₃], and the tris-azide CLA benzene-1,3,5-triyl tris(4-azido-2,3,5,6-tetrafluorobenzoate).

multilayer devices.^{9–11} This is realized by either attaching reactive substituents to the polymer side chains or by adding a molecular cross-linking agent (CLA) to the polymer solution. After layer deposition, a thermal or optical stimulus can initiate reactions to form covalent bonds between adjacent polymer chains, resulting in a cross-linked polymer network. As a measure of the success of approaching layer insolubility, one can determine the retention of the layer after immersion in a solvent under specified conditions. To achieve high retention, thermal cross-linking in many cases requires long annealing times or high temperatures. While long annealing times are inefficient for mass production of devices, high temperatures can cause damage to the polymer or to an underlying flexible substrate.¹² In contrast, photo-cross-linking requires neither long annealing times nor high temperatures in order to achieve high layer retention and can be realized at room temperature within seconds, although it is important to ensure that neither the irradiation used nor the photochemistry of the cross-linking group leads to the degradation of the performance of any of the active materials.¹³ One key tool that we use here is the photolysis of fluoroaryl azides to give highly reactive singlet nitrenes,^{14,15} which can be inserted into the C–H bonds of the polymer alkyl side chains.^{9,16,17} By using a CLA with multiple azide moieties, this reaction leads to cross-linking, and high layer retention can be achieved at comparably low CLA concentration. This is of importance since high CLA loading can disturb the interchain packing structure of the polymer and thus lower the charge carrier mobility and device performance.^{9,13} While cross-linking of neat polymers is well established, the retention of molecular dopants in cross-linked

polymer layers with respect to immersion in solvents has yet to be investigated.

Previous studies have demonstrated that the addition of molecular dopants to polymer layers can itself induce high solvent resistance. Jacobs et al. observed doping-induced layer retention in a wide range of solvents for poly(3-hexylthiophene-2,5-diyl) (P3HT) sequentially doped with 2,3,5,6-tetrafluoro-7,7,8,8-tetracyanoquinodimethane (F₄TCNQ).¹⁸ Other studies on P3HT doped with tris(pentafluorophenyl)borane (BCF), F₄TCNQ-doped poly[2,5-bis(3-dodecyl-2-thienyl)-thieno(3,2-*b*)thiophene] (C12-PBTTT), and poly[2-methoxy-5-(2'-ethylhexyloxy)-*p*-phenylene vinylene] (MEH-PPV) have found aggregation of polymer chains already in solution after adding the molecular dopant to the polymer solution.^{19–22} We have recently reported that the tetrafunctional *n*-dopant tetrakis[(4-(1,3-dimethyl-2,3-dihydro-1*H*-benzo[*d*]imidazol-2-yl)phenoxy)methyl]methane largely insolubilizes a thiophene-fused benzodifurandione-based oligo(*p*-phenylenevinylene)-*co*-thiophene polymer in the original deposition solvent and have attributed this to the network of electrostatic interactions formed by the resulting tetracation and negatively charged polymer chain segments.²³

Here, we focus on the two above-mentioned mechanisms for enhancing the resistance of doped polymer layers against exposure to solvent, while also retaining the dopants: pre-aggregation-induced and cross-linking-induced layer retention are compared to clarify the interplay of these effects and to show their potential for the fabrication of multi-heterolayer structures. First, using 1,2,4,5,7,8-hexafluoro-11,11,12,12-tetracyanonaphtho-2,6-quinodimethane (F₆TCNNQ) as a molecular *p*-dopant, we show that the layer retention of P3HT can

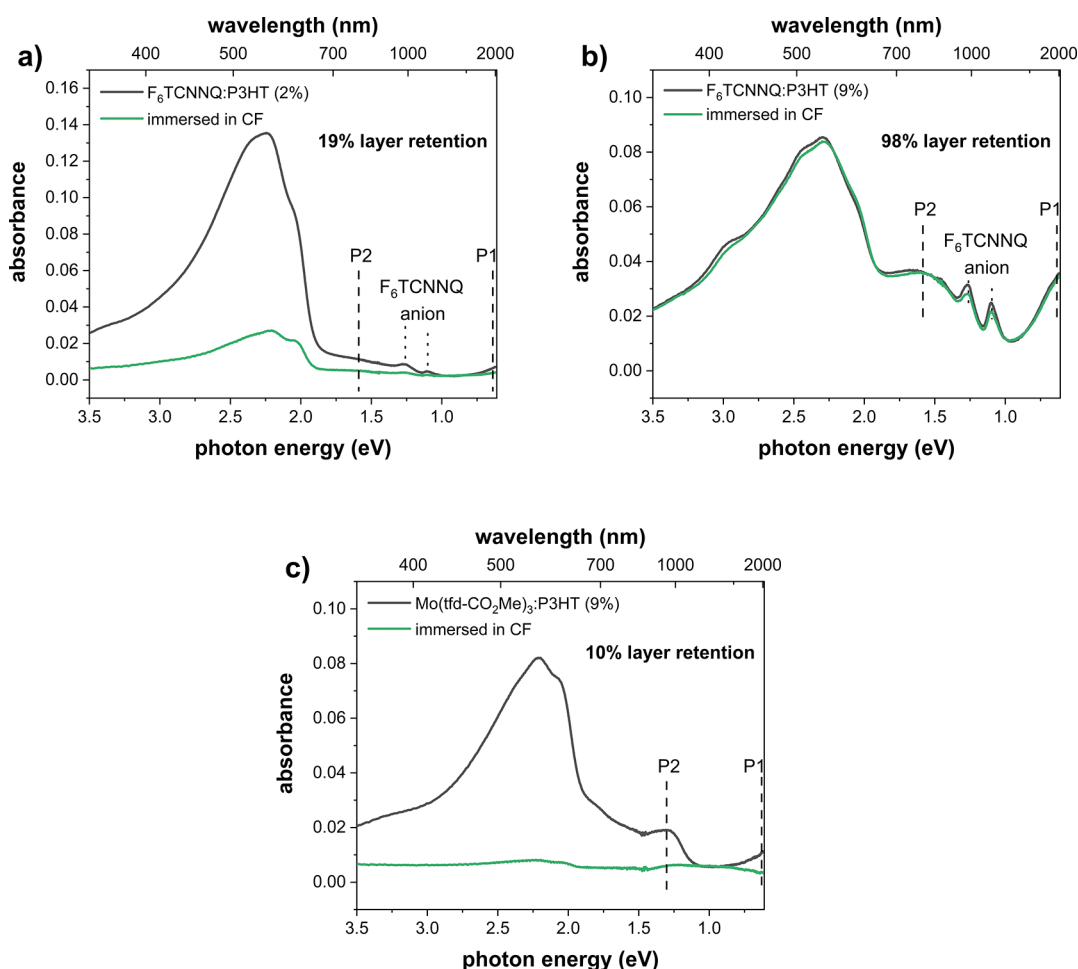


Figure 2. Optical absorption spectra of (a) 2%, (b) 9% F_6TCNNQ -doped P3HT layer, and (c) 9% $Mo(tfd-CO_2Me)_3$ -doped P3HT layer before and after immersing the layer for 10 min in CF. It should be noted here that doped, aggregated P3HT chains can exhibit absorption features at 1.3 and 1.6 eV (labeled P2).¹⁹

be enhanced [with up to 98% retention after 10 min immersion in chloroform (CF)] by increasing the dopant concentration and thus the amount of pre-aggregated P3HT chains in solution. In contrast, doping of P3HT with the molecular p-dopant molybdenum tris[1-(methoxycarbonyl)-2-(trifluoromethyl)ethane-1,2-dithiolene] [$Mo(tfd-CO_2Me)_3$] with the same dopant concentration leads to a layer retention of only 10%. The difference observed between $Mo(tfd-CO_2Me)_3$ - and F_6TCNNQ -doped P3HT is attributed to a lower ionization efficiency of $Mo(tfd-CO_2Me)_3$ in P3HT than of F_6TCNNQ . This results in a smaller change in material polarity and thus less polymer pre-aggregation, thereby compromising the solvent resistance of $Mo(tfd-CO_2Me)_3$ -doped P3HT layers.

For the cross-linking approach, we use the photo-activated CLA benzene-1,3,5-triyl tris(4-azido-2,3,5,6-tetrafluorobenzoate).^{13,24} This CLA allows for enhanced solvent resistance of F_6TCNNQ -doped P3HT layers even at low dopant concentration, as well as of P3HT layers that are doped with the comparably less efficient p-dopant $Mo(tfd-CO_2Me)_3$. The chemical structures of all compounds are depicted in Figure 1. By comparing the solvent resistance of doped P3HT and poly[2,5-bis(3-tetradecylthiophen-2-yl)thieno[3,2-*b*]-thiophene] (PBTTT), we find that the excessive pre-aggregation in solution prevents proper incorporation of the CLA between polymer chains, thereby reducing the number of

available polymer side chains to undergo the cross-linking reaction. The results show that the pre-aggregation in solution and the use of CLAs must be carefully balanced to achieve high solvent resistance of doped polymer layers.

EXPERIMENTAL SECTION

Regioregular ($M_w = 50\text{--}100$ kg/mol, regioregularity > 90%) and regiorandom P3HT were purchased from Sigma-Aldrich GmbH. PBTTT ($M_w > 50$ kg/mol) was purchased from Merck KGaA, and F_6TCNNQ was obtained from Novaled GmbH. $Mo(tfd-CO_2Me)_3$ and the tris-azide CLA¹³ were synthesized as described elsewhere. Stock solutions with concentrations of 2 mg mL⁻¹ of the semiconductors and dopants were prepared under a nitrogen atmosphere in an inert gas box using dried CF for doped P3HT and chlorobenzene (CB) for doped PBTTT solutions, respectively. PBTTT solutions were kept on a hot plate at 100 °C in order to prevent formation of aggregates.²¹ Cross-linked layers were fabricated in an inert gas box by adding the tris-azide molecule to the undoped solution, unless otherwise stated. Afterward, the dopant solution was added to the solution of the polymer and cross-linker. The reported dopant (cross-linker) concentration c , given as a percentage, is defined as $c = N_D / (N_D + N_P)$, with the number of dopant (cross-linker) molecules N_D and the number of polymer monomer units N_P as contained in the solution. Thin layers (7–20 nm) were prepared by spin-coating using a standard laboratory spin-coater at 2000 rpm for 1 min on either solvent cleaned glass (for optical absorption spectroscopy and scanning force microscopy) or ITO substrates [for ultraviolet photoelectron spectroscopy (UPS)]. Since small

dopant molecules can be removed during the spin-coating process, the nominal dopant concentration was cross-checked by estimating the fluorine-to-sulfur atomic ratios using X-ray photoelectron spectroscopy (XPS) intensities for 9%-doped P3HT layers. For Mo(tfd-CO₂Me)₃- and F₆TCNNQ-doped P3HT, the XPS data indicated dopant concentrations of 7 and 6%, respectively, both of which are in reasonable quantitative agreement with the nominal dopant concentrations. Photo-cross-linking was realized by exposing the respective layers to a UV lamp (wavelength: 254 nm) for 4 min. To test the layer retention, P3HT and PBTTT layers were immersed in CF or CB, respectively, for 10 min and dried with nitrogen gas afterward. Note that the harsh conditions of solvent immersion were intentionally chosen to allow estimation of a lower limit value for retention of the doped layers. When forming multi-heterolayer structures via spin-coating, the relevant (underlying) layer is exposed for only a few seconds to the solvent used for deposition of the second layer.

Optical absorption spectroscopy was carried out using a Lambda 950 UV–vis–near-infrared (NIR) spectrophotometer (PerkinElmer, Inc.). The layer retention was determined by the relative change in the optical absorption at the most prominent peak (at a photon energy of ≈ 2.2 – 2.3 eV) after immersing the layer in the respective solvent via $\left(1 - \frac{I_a - I_b}{I_b}\right) \cdot 100\%$ (I_b and I_a being the optical absorbances before and after immersing the layer in solvent, respectively). Note that the signal at 861 nm appearing in some spectra is an artifact stemming from the detector and grating change of the spectrometer used. To account for these offsets in the recorded spectra, the NIR region (>861 nm) was aligned to the visible region (319–861 nm) by shifting the absorbance up or down with a constant offset.

Scanning force microscopy was performed using a Bruker Dimension Icon system. Surface topography images were measured in the PeakForce-tapping mode, using the ScanAsyst module and ScanAsyst-Air cantilevers.

Conductivity measurements were carried out under a nitrogen atmosphere using pre-patterned glass substrates with an interdigitated ITO electrode structure with varying channel length, purchased from Ossila Ltd. Current–voltage (I – V) measurements were conducted using an Ossila I – V test board and a Keithley 2635A source meter.

UPS measurements were performed using a non-monochromated helium-gas discharge lamp (21.22 eV) with a low photon flux (attenuated using an 800 nm aluminum filter) to prevent radiation damage of the samples. The spectra were collected in normal emission. An Omicron EA125 hemispherical electron energy analyzer with a pass energy of 5 eV was used. To clear the analyzer work function, a bias of -10 V was applied to the sample for secondary electron cutoff spectra.

RESULTS AND DISCUSSION

A P3HT layer spin-coated from a CF solution can readily be redissolved when immersed in CF for 10 min. In contrast, an F₆TCNNQ-doped P3HT layer deposited from CF solution remains—to some extent—on the substrate after immersion in CF, as can be inferred from the optical absorption spectra in Figure 2a,b. The spectral features at 2.1 and 2.2 eV can be assigned to optical signatures of charge-neutral P3HT with aggregated chains.^{25,26} The peaks labeled P1 and P2 are characteristic of positive polarons of P3HT; they have previously been reported in the ranges of 0.4–0.5 eV (P1) and 1.3–1.7 eV (P2), respectively.^{19,27–29} It has also been shown that the P2 transition can be split into two features, that is, at 1.3 and 1.65 eV; this has been attributed to interchain interactions between doped aggregated P3HT chains.¹⁹ For P3HT doped with F₆TCNNQ, details of this splitting are obscured by a spectral overlap with the transitions of the F₆TCNNQ radical anions, as labeled in the figures.

The layer retention (defined here as the relative change in the optical absorption at 2.2 eV after immersing the sample 10 min in CF) of a 2% F₆TCNNQ-doped P3HT layer is about 19%. For a dopant concentration of 9%, the layer retention increases to 98%. Moreover, only negligible changes in the ratios between the absorbances of optical absorption features of neutral P3HT, P3HT polarons, and F₆TCNNQ anions can be observed after the immersion, also indicating high dopant retention. To better rationalize these observations, we recall why a polymer layer becomes dissolved or remains mostly unaffected by solvent immersion. In general, the miscibility of the two components (here a polymer and a molecular solvent) depends on temperature (T) and the solution composition. By mixing a polymer and a solvent, the entropy S of the system is increased. Under the condition of constant pressure, intimate contact formation between the two different components releases or requires energy, leading to a change in enthalpy H . The balance between S and H is related to the Gibbs free energy G , via $G = H - TS$. The polymer and solvent are, therefore, miscible if the G of the polymer–solvent composition is smaller than that of the individual components,³⁰ until the saturation concentration c_{sat} is reached. In the case of an extremely dilute solution, the individual polymer chains are separated from each other. When increasing the polymer concentration c in the solvent, the polymer chains also start to interact with each other. At c_{sat} the individual chains overlap significantly and start to form aggregates.^{31–33} Once the aggregates are formed, they cannot be dissolved by adding more solvent ($c < c_{\text{sat}}$). To re-dissolve the aggregated polymer chains, a gain in S is required, which can be realized by increasing T , for instance. Therefore, the solubility of a polymer depends on the balance between intermolecular interaction among polymer chains and interactions of the polymer with the solvent molecules. Since most semiconductor polymers, and certainly those considered here, are based on units with similar electronegativities, they can mostly be considered weakly polar. Intrinsically weakly polar polymers can dissolve well in the weakly polar solvents, such as CF, due to a small overall change in enthalpy. In contrast, weakly polar polymers avoid interacting with polar solvents, such as water, by minimizing contact, and therefore show low solubility in polar solvents.

With the aforementioned in mind, the retention of F₆TCNNQ-doped P3HT layers can be explained by a change in overall polarity due to the charge transfer involved in doping. Adding F₆TCNNQ to P3HT solution leads to the formation of positively charged polymer chain segments (positive polarons) and F₆TCNNQ anions. The increase in compound polarity (which increases with increased dopant concentration) results in an unfavorable interaction with the weakly polar CF solvent molecules. As a result, c_{sat} is decreased and the amount of polymer aggregates in solution increases. Once formed, the aggregates cannot be re-dissolved by lowering c , as described above. Consequently, the solvent resistance of a doped polymer layer increases with the amount of pre-aggregation in solution. Besides layer retention after immersion in CF and dichlorobenzene, F₆TCNNQ-doped P3HT layers also exhibited good resistance against dissolution when immersed in more polar solvents such as ethanol. This can be explained by an edge-on orientation of the P3HT alkyl side chains relative to the layer surface, as usually observed for semi-crystalline polymers with alkyl side chains.³⁴ The surface-exposed weak polar C–H side-chain groups are poorly soluble

in ethanol and avoid interaction with the polar solvent molecules, thus preventing solvent diffusion into the bulk of the layer where the polar polymer polarons and dopant anions reside.

The proposition that polymer pre-aggregation in solution leads to improved layer retentions is supported by optical absorption spectra of a neat (undoped) PBTBT layer before and after immersion in CB for 10 min (see Figure S1, Supporting Information). This polymer tends to aggregate in solution within a few seconds when cooled down to room temperature. This is indicated by a color change of the solution from bright to dark red.^{21,35} The pronounced pre-aggregation of neat PBTBT in solution results in a noteworthy retention of about 24% in our experiments.

Even though the retention of F₄TCNQ, F₄OCTCNQ, Mo(tfd)₃, and DDQ-doped P3HT [F₄OCTCNQ = 2,3,5,6-tetrafluoro-7-octyloxycarbonyl-7,8,8-tricyanoquinodimethane; Mo(tfd)₃ = molybdenum tris[1,2-bis(trifluoromethyl)ethane-1,2-dithiolene]; and DDQ = 2,3-dichloro-5,6-dicyanoquinodimethane] layers after exposure to solvents has been observed in previous studies,³⁶ pre-aggregation (and thus doping-induced) layer retention depends on the dopant. As shown in Figure 2c, doping of P3HT with Mo(tfd-CO₂Me)₃ results in a layer that has a low retention after immersion in CF. While that of a 9% F₆TCNNQ-doped P3HT layer was about 98%, the retention of a 9% Mo(tfd-CO₂Me)₃-doped P3HT layer is only about 10%. This can be explained by a lower oxidation strength of Mo(tfd-CO₂Me)₃ (reduction potential of +0.12 V vs FeCp₂⁺/FeCp₂³⁷) than that of F₆TCNNQ (reduction potential of +0.17 V vs FeCp₂⁺/FeCp₂³⁸), which results in a lower ionization efficiency and thus less aggregation in solution. The optical absorption spectra reveal that the relative intensity of the polaron features in relation to the neutral P3HT feature (at ≈2.2 eV) for 9% F₆TCNNQ-doped P3HT is higher than for 9% Mo(tfd-CO₂Me)₃-doped P3HT. This indicates that doping P3HT with F₆TCNNQ leads to more positive polarons per dopant molecule than doping with Mo(tfd-CO₂Me)₃. Additionally, scanning force microscopy confirms that there is less aggregation in a 9% Mo(tfd-CO₂Me)₃-doped P3HT layer compared to that in 9% F₆TCNNQ-doped P3HT. As can be seen in Figure 3a,b, the

addition of 2% F₆TCNNQ to P3HT leads to the formation of aggregates in the form of not only fibrils but also rod-like structures. These structures become larger when increasing the dopant concentration to 9% (see Figure 3c). In contrast to that, a Mo(tfd-CO₂Me)₃-doped P3HT film at the same dopant concentration exhibits smaller-sized aggregates (see Figure 3d). Notably, further enhancing the overall polarity by increasing the Mo(tfd-CO₂Me)₃ concentration in P3HT beyond 9% did not lead to higher layer retention. Therefore, further contributions need to be considered.

Although electron transfer between P3HT and Mo(tfd-CO₂Me)₃ occurs, it might be possible that this happens only in the specific domains of the P3HT layer. It has already been observed that the IE of aggregated domains in P3HT is lower than that of the amorphous P3HT domains.^{39,40} The difference has been estimated to be around 0.3 eV and used to explain the unfavorable charge transfer between non-aggregated P3HT and F₄TCNQ.³⁹ Noriega et al. suggested that the amorphous domains in regioregular P3HT (rr-P3HT) can be approximated by regiorandom P3HT (rra-P3HT).³⁴ According to cyclic voltammetry data, the IEs of aggregated and amorphous P3HT domains are about 4.99 and 5.25 eV, respectively.⁴¹ Under the premise that the ferrocene/ferrocenium energy level is 4.8 eV below the vacuum level, the corresponding EA of Mo(tfd-CO₂Me)₃ is approximately 4.9 eV.^{42,43} Thus, while electron transfer between Mo(tfd-CO₂Me)₃ and aggregated P3HT can occur, charge transfer with the amorphous P3HT domains is energetically unfavorable. In agreement with this, previous studies have shown that Mo(tfd-CO₂Me)₃ does not dope rra-P3HT.⁴⁴ Therefore, we propose that the amorphous domains in P3HT are mostly unaffected by this molecular dopant, resulting in a local weak polarity. Consequently, these amorphous domains are still soluble in CF. In contrast, F₆TCNNQ is able to dope rra-P3HT, as can be seen in Figure S2 in the Supporting Information. This might seem to be in contradiction to a recently published work, showing that F₆TCNNQ does not dope amorphous P3HT regions while Mo(tfd-CO₂Me)₃ does.⁴⁵ In fact, the different layer and doping processing applied in that study (high-temperature rubbing and incremental concentration doping to make oriented doped P3HT layers) result in different layer dynamics and kinetics and, therefore, do not allow a direct comparison.

Doping-induced pre-aggregation in solution thus represents a simple mechanism to enhance the solvent resistance of doped polymer layers. However, the dopant of choice needs to promote the formation of aggregates already at sufficiently low dopant concentrations. Otherwise, the morphology of the polymer layer can be disrupted, and the charge carrier mobility can be reduced. Besides its ability to act as a strong oxidizing/reducing molecule, the dopant's size and solubility in the casting solution play a crucial role. Bulkiness and the formation of solvation shells can result in long distances between the dopant and polymer, thus suppressing the interaction between both⁴⁶ and enabling dissolution of formed layers.

The solvent resistance of doped polymer layers was studied via the covalent cross-linking approach. The availability of multiple azido groups per CLA enables high layer retention capability even at a low cross-linker concentration.^{9,13} In agreement, we find that the retention of a 2% F₆TCNNQ-doped P3HT layer after CF immersion increased from 19% (no CLA) to 98% when adding 2% photo-reactive tris-azide cross-linker (each molecule bearing three azido groups) to the

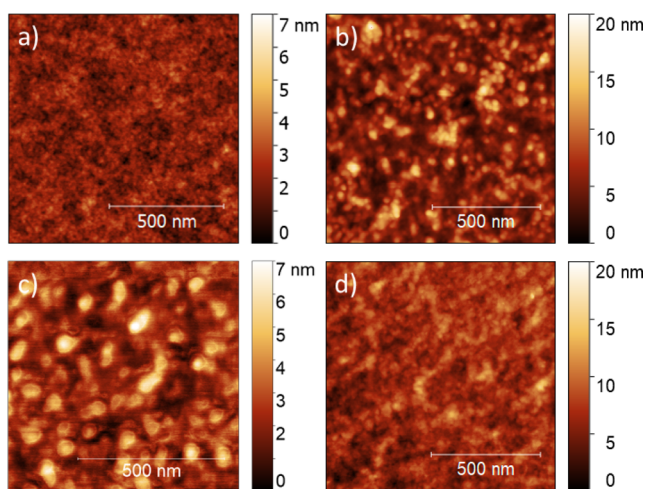


Figure 3. Scanning force microscopy images of (a) undoped P3HT, (b) 2% F₆TCNNQ-doped P3HT, (c) 9% F₆TCNNQ-doped P3HT, and (d) 9% Mo(tfd-CO₂Me)₃-doped P3HT.

P3HT solution and subsequently exposing to UV irradiation (F_6TCNNQ was added to the solution afterward) (see Figures 2a and 4, respectively).

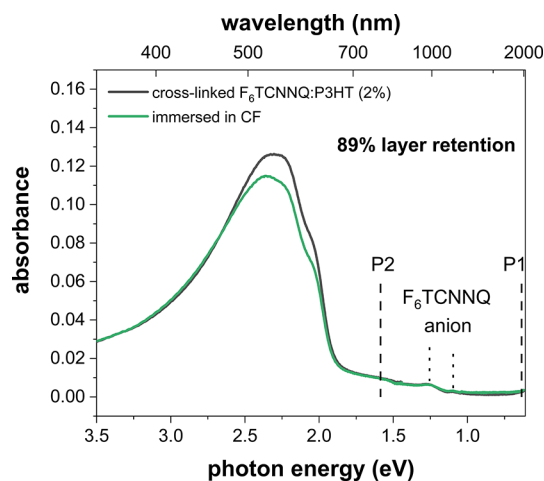


Figure 4. Optical absorption spectra of a cross-linked, 2% F_6TCNNQ -doped P3HT layer (2% cross-linker concentration) before and after immersing the layer for 10 min in CF.

While there is some loss of neutral P3HT (absorption at 2.2 eV), the absorption signal of P3HT polarons and F_6TCNNQ anions was not lowered after immersing the cross-linked layer in CF, indicating also an improved dopant retention compared to that of the non-cross-linked 2% F_6TCNNQ -doped P3HT layer. This is seemingly enabled by the highly cross-linked polymer network that traps the dopant molecules.

Despite a gain in layer retention on cross-linking the doped polymer, a significantly improved retention of the dopant upon thermal stress was not observed. Regardless of whether the F_6TCNNQ -doped P3HT layers were cross-linked or not, the P3HT polaron and F_6TCNNQ anion transitions decreased after annealing the layers at 60 °C for 10 min, as displayed in the optical absorption spectra in Figure S3. The signals further attenuated when turning to 90 °C, indicating diffusion and desorption of F_6TCNNQ for both the layers.

Next, we turn toward the issue of polymer pre-aggregation in solution. While doping-induced pre-aggregation in solution has

been shown to enhance the retention of doped P3HT layers, the formation of aggregates could lower the cross-linking capability¹⁷ of the tris-azide molecule. As displayed in Figure 5, the retention is significantly lower for a layer made from a blend solution in which (i) the cross-linker is added to the (freshly made) dopant/polymer solution than for a layer (ii) in which the dopant is added to the polymer:cross-linker solution. In case (i), pre-aggregation in $Mo(tfd-CO_2Me)_3$:P3HT blend solution occurs due to the electron transfer. We suggest that the bulky CLA cannot effectively be inserted between the aggregated polymer chains, neither at the solution-casting stage nor after layer formation. In consequence, the cross-linking within aggregates is poor. This results in the removal of neutral and doped P3HT domains upon solvent immersion, as indicated by a decreased absorbance of the polymer layer after immersion in CF. The ratio of absorbance at P2 (transition of positively charged P3HT) to that at ≈ 2.2 eV (transition of neutral P3HT) is decreased by 13% after immersion in CF. In case (ii), the CLA molecules can effectively associate in non-aggregated P3HT chains in solution before the addition of $Mo(tfd-CO_2Me)_3$ and concomitant doping. The ratio of absorbance at P2 to that at ≈ 2.2 eV is decreased by only 8% after immersion in CF, indicating that the loss of dopants is less pronounced.

The negative effect of pre-aggregation on the cross-linking capability was also observed for undoped rra-P3HT, rre-P3HT, and PBTTT, using the same CLA concentration of 2% in all the cases. The layer retention of cross-linked rra-P3HT (amorphous, low tendency to aggregate⁴⁷) is 94%, see Figure S4a. When cross-linking rre-P3HT (made up of amorphous and aggregated domains⁴⁷), the layer retention is 85%, see Figure S4b. Cross-linking of PBTTT (high tendency to aggregate^{21,35}) results in a layer retention of only 74%, as shown in Figure S5a in the Supporting Information. Formation of aggregates in solution thus suppress the cross-linking capability of the tris-azide molecule in general. Due to this, no retention of dopants and, thus, PBTTT polarons upon solvent immersion can be observed. As shown in Figure S5b, the optical absorption features of polarons in a cross-linked 9% $Mo(tfd-CO_2Me)_3$ -doped PBTTT layer vanished after immersion in CB. The dissolution of $Mo(tfd-CO_2Me)_3$ and PBTTT polarons may also be explained by a low ionization efficiency of

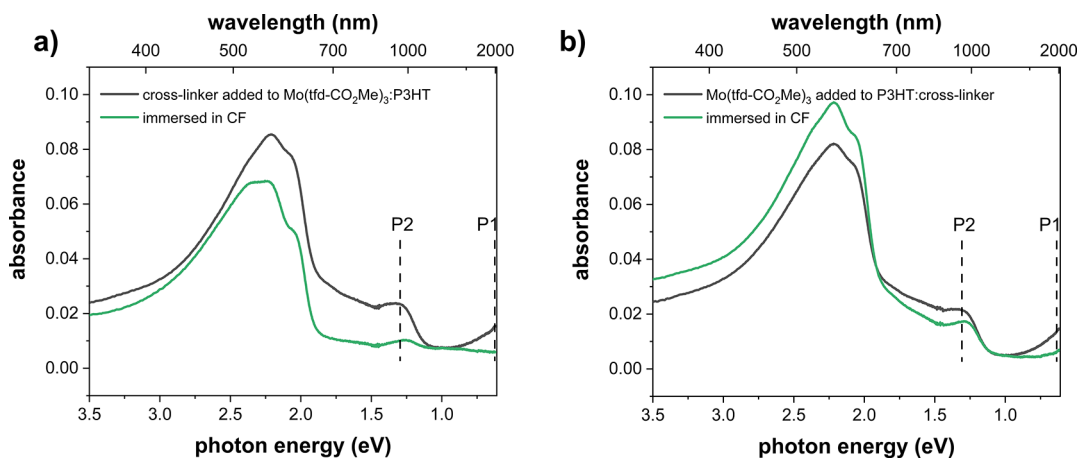


Figure 5. Optical absorption spectra of a 9% $Mo(tfd-CO_2Me)_3$ -doped P3HT layer (2% cross-linker concentration) before and after immersing the layer for 10 min in CF. While in (a), the cross-linker was added to the dopant/polymer blend solution, in (b), the dopant was added to the polymer/cross-linker blend solution prior to layer formation.

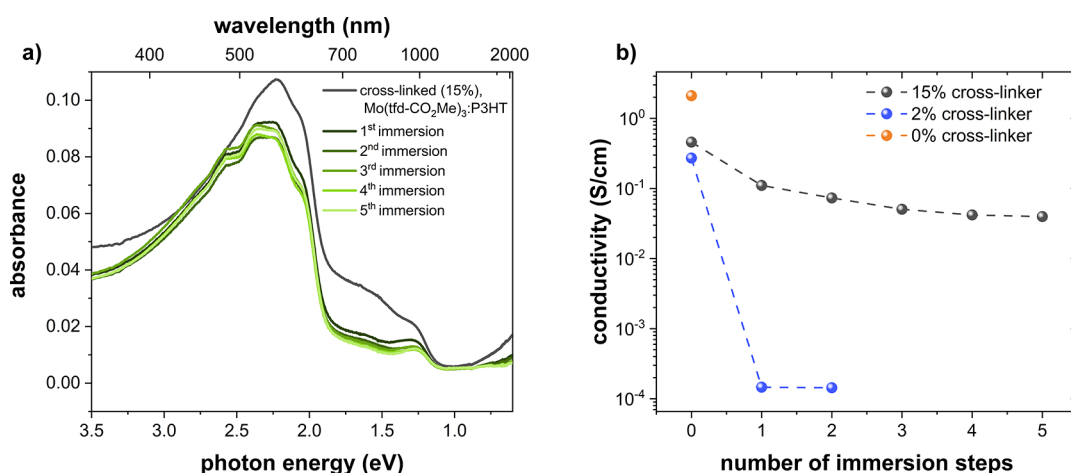


Figure 6. (a) Optical absorption spectra of a 9% $\text{Mo}(\text{tfd-CO}_2\text{Me})_3$ -doped P3HT layer with 15% cross-linker concentration before and after immersing the layer in CF. (b) Bulk conductivity of 9% $\text{Mo}(\text{tfd-CO}_2\text{Me})_3$ -doped P3HT layers with varying cross-linker content before and after immersing in CF. The layer thicknesses were 19 nm (at 15% cross-linker concentration) and 16 nm (at 2% cross-linker concentration) before immersion. Subsequent immersion steps lead to final thicknesses of 13 nm (at 15% cross-linker concentration) and 9 nm (at 2% cross-linker concentration).

$\text{Mo}(\text{tfd-CO}_2\text{Me})_3$ (EA ≈ 5.0 eV, determined by inverse photoelectron spectroscopy)⁸ in PBTTT (IE ≈ 5.15 eV, determined by UPS).⁴⁸ This leads to a larger fraction of neutral $\text{Mo}(\text{tfd-CO}_2\text{Me})_3$ molecules than of $\text{Mo}(\text{tfd-CO}_2\text{Me})_3$ anions in the doped polymer layer. Once the doped layer is immersed, neutral $\text{Mo}(\text{tfd-CO}_2\text{Me})_3$ molecules are dissolved, leading to a shift in the chemical equilibrium (with an equilibrium constant of $\frac{[\text{Mo}(\text{tfd-CO}_2\text{Me})_3^-][\text{PBTTT}^+]}{[\text{Mo}(\text{tfd-CO}_2\text{Me})_3][\text{PBTTT}]}$). To maintain equilibrium, $\text{Mo}(\text{tfd-CO}_2\text{Me})_3$ anions are converted to neutral $\text{Mo}(\text{tfd-CO}_2\text{Me})_3$ molecules that are eventually dissolved as well. As a result, no signatures of PBTTT polarons can be observed in the optical absorption spectrum upon solvent immersion.

By reducing the extent of pre-aggregation (by adding the molecular dopant to the polymer:CLA solution), the layer retention can be further enhanced by increasing the amount of CLA. As noted above, the relative intensity of the P2 transition to the neutral polymer transition decreased by 8% for a cross-linked $\text{Mo}(\text{tfd-CO}_2\text{Me})_3$ -doped P3HT layer (with 2% CLA) after immersion in CF. When increasing the CLA concentration to 15%, optical absorption spectra reveal that the relative intensity of P2 decreases by only 2% after immersing the layer in CF for 10 min (see Figure 6a). An additional immersion step leads to a further loss of dopants and thus polarons. However, subsequent immersion steps do not lead to further losses of neutral and doped polymers of the layer. The optical results are consistent with conductivity data: as displayed in Figure 6b, the conductivity of the doped layer with 15% CLA concentration drops in total by 1 order of magnitude after five solvent immersion steps, while, in contrast, the conductivity of the doped layer with only 2% CLA concentration decreases by 3 orders of magnitude already after the first immersion step. Given that harsh conditions of solvent exposure have been chosen, representing a “worse-case” scenario, a drop in conductivity by 1 order of magnitude can be considered sufficiently stable for multi-heterolayer device application. The drop in conductivity is most likely induced by the loss of dopants (see Figure 6a) and thus, reduced charge carrier density, although a suppressed charge carrier mobility may also play a role; in particular, it cannot be excluded that solvent molecules are able to diffuse into the

doped polymer layer during immersion and perturb the layer microstructure with concomitant adverse effects on mobility. The better-preserved conductivity of the 15% CLA layer compared to that of the 2% CLA layer is in line with a more densely cross-linked polymer network that leads to an improved layer retention and simultaneously facilitates effective trapping of dopant molecules. Notably, the layer retentions of the undoped cross-linked P3HT layer with 2 and 15% CLA concentrations are rather similar (85 and 88%, respectively; see Figure S6, Supporting Information). With respect to the $\text{Mo}(\text{tfd-CO}_2\text{Me})_3$ -doped P3HT layers, this suggests that $\text{Mo}(\text{tfd-CO}_2\text{Me})_3$ is also involved in cross-linking reactions. Linkage might be enabled by methyl groups of $\text{Mo}(\text{tfd-CO}_2\text{Me})_3$, but no direct evidence for this has been obtained so far. It should be noted that the addition of the CLA leads to a reduced conductivity. This can be explained by the CLA inducing structural intermolecular disorder in the polymer matrix, leading to a reduction in the charge carrier mobility. The conductivity of a non-cross-linked 9% $\text{Mo}(\text{tfd-CO}_2\text{Me})_3$ -doped P3HT layer is 2.1 S/cm. After adding 2% CLA, the conductivity is reduced to 0.3 S/cm. A reduction in conductivity is also observed for a F_6TCNNQ -doped P3HT layer. A non-cross-linked 2% F_6TCNNQ -doped P3HT layer gives a conductivity of 6×10^{-3} S/cm. Adding 2% CLA decreases the conductivity to 1×10^{-3} S/cm. A comparison to 9% F_6TCNNQ -doped P3HT is not made at this point since the conductivity was found to saturate at this dopant concentration. Since this dopant concentration already provides a high layer retention of 98%, the addition of the CLA would not have resulted in significantly improved layer retention but might, rather, be anticipated to afford a decreased conductivity, as discussed above.

Finally, UPS data confirm that the electronic structures of pristine P3HT and P3HT with 15% CLA concentration are almost identical (see Figure S7, Supporting Information). SFM data in Figure 7 reveal a slightly increased surface inhomogeneity at such a high cross-linker concentration for P3HT layers, indicated by an increased root mean square value from 0.51 to 0.83 nm, but conductivity data do not indicate a significant impact on carrier mobility (assuming that the carrier concentration is not modified by cross-linking). For 9%

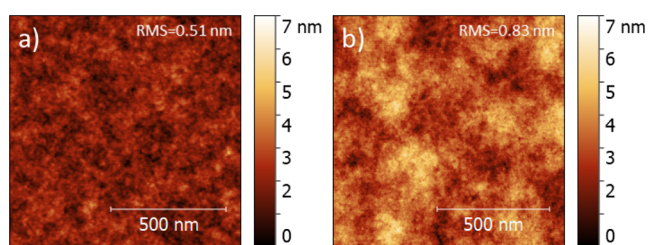


Figure 7. Scanning force microscopy images of (a) P3HT and (b) cross-linked P3HT layer; 15% cross-linker concentration.

Mo(tfd-CO₂Me)₃-doped P3HT layers, with 2 and 15% CLA concentrations, we measure conductivity values of 0.3 and 0.5 S/cm, respectively.

CONCLUSIONS

In this work, we have investigated two different mechanisms that improve the resistance of molecularly doped polymer semiconductor layers against solvent dissolution, one being the doping-induced pre-aggregation in solution and the other using a photo-reactive agent for covalent cross-linking. In the first case, the addition of molecular dopants to polymer solution leads to an overall change in polarity due to the charge transfer involved in doping, resulting in an unfavorable interaction between the polar compounds and weakly polar solvent molecules. While doping of P3HT with F₆TCNNQ results in a high layer retention of 98%, Mo(tfd-CO₂Me)₃-doped P3HT layers are still soluble even at high dopant concentrations. This was assigned to a lower ionization efficiency of Mo(tfd-CO₂Me)₃ in P3HT than of F₆TCNNQ, resulting in reduced aggregation formation in Mo(tfd-CO₂Me)₃-doped P3HT solution. Thus, doping-induced layer retention does not represent a universal tool to provide high resistance against solvent dissolution but depends on the dopant and its capability to promote the formation of aggregates.

In contrast, cross-linking of organic layers with the photo-reactive tris-azide cross-linker has provided high retention of both F₆TCNNQ- and Mo(tfd-CO₂Me)₃-doped P3HT layers even at low dopant concentration. While a 2% F₆TCNNQ-doped P3HT layer provides a layer retention of 19%, cross-linking of a 2% F₆TCNNQ-doped P3HT layer leads to an enhanced layer retention of 98%. However, pre-aggregation in solution (prior to adding the cross-linker) must be prevented to achieve high solvent resistance of doped polymer layers. Taking this into account, a highly cross-linked polymer network can be realized, which seemingly traps the dopant molecules and improves the dopant retention against solvent dissolution, resulting in a largely retained electrical conductivity of the doped polymer layer. Likewise, the formation of new covalent bonds between the tris-azide cross-linker and the methyl groups in Mo(tfd-CO₂Me)₃ could not be ruled out. This serves to steer future research efforts, especially in terms of the synthesis of molecular dopants with more C–H bonds, combined with a cross-linker containing a larger number of azide moieties to increase the chance of the reaction and, therefore, improve the dopant retention.

ASSOCIATED CONTENT

Supporting Information

The Supporting Information is available free of charge at <https://pubs.acs.org/doi/10.1021/acs.chemmater.2c03262>.

Optical absorption and photoelectron spectroscopy spectra (PDF).

AUTHOR INFORMATION

Corresponding Author

Norbert Koch – *Institut für Physik & IRIS Adlershof, Humboldt-Universität zu Berlin, D-12489 Berlin, Germany; Helmholtz-Zentrum Berlin für Materialien und Energie GmbH, D-12489 Berlin, Germany; orcid.org/0000-0002-6042-6447; Email: norbert.koch@physik.hu-berlin.de*

Authors

Dominique Lungwitz – *Institut für Physik & IRIS Adlershof, Humboldt-Universität zu Berlin, D-12489 Berlin, Germany; orcid.org/0000-0003-1662-2114*

Ahmed E. Mansour – *Institut für Physik & IRIS Adlershof, Humboldt-Universität zu Berlin, D-12489 Berlin, Germany; Helmholtz-Zentrum Berlin für Materialien und Energie GmbH, D-12489 Berlin, Germany*

Yadong Zhang – *School of Chemistry and Biochemistry and Center for Organic Photonics and Electronics, Georgia Institute of Technology, Georgia 30332-0400, United States; Renewable and Sustainable Energy Institute, University of Colorado Boulder, Boulder, Colorado 80303, United States*

Andreas Opitz – *Institut für Physik & IRIS Adlershof, Humboldt-Universität zu Berlin, D-12489 Berlin, Germany; orcid.org/0000-0002-3214-8398*

Stephen Barlow – *School of Chemistry and Biochemistry and Center for Organic Photonics and Electronics, Georgia Institute of Technology, Georgia 30332-0400, United States; Renewable and Sustainable Energy Institute, University of Colorado Boulder, Boulder, Colorado 80303, United States; orcid.org/0000-0001-9059-9974*

Seth R. Marder – *School of Chemistry and Biochemistry and Center for Organic Photonics and Electronics, Georgia Institute of Technology, Georgia 30332-0400, United States; Renewable and Sustainable Energy Institute, University of Colorado Boulder, Boulder, Colorado 80303, United States; Department of Chemical and Biological Engineering and Department of Chemistry, University of Colorado Boulder, Boulder, Colorado 80303, United States; orcid.org/0000-0001-6921-2536*

Complete contact information is available at: <https://pubs.acs.org/10.1021/acs.chemmater.2c03262>

Author Contributions

The manuscript was written through contributions of all authors. All authors have given approval to the final version of the manuscript.

Notes

The authors declare no competing financial interest.

ACKNOWLEDGMENTS

This work was supported by the Deutsche Forschungsgemeinschaft (DFG)—project nos. 239543752 and 182087777—SFB 951, and the National Science Foundation (through DMR-807797, the DMREF program, DMR-1729737), and ONR (through N00014-20-1-2587).

REFERENCES

- (1) Murawski, C.; Fuchs, C.; Hofmann, S.; Leo, K.; Gather, M. C. Alternative p-Doped Hole Transport Material for Low Operating Voltage and High Efficiency Organic Light-Emitting Diodes. *Appl. Phys. Lett.* **2014**, *105*, 113303.
- (2) Lüssem, B.; Keum, C. M.; Kasemann, D.; Naab, B.; Bao, Z.; Leo, K. Doped Organic Transistors. *Chem. Rev.* **2016**, *116*, 13714.
- (3) Lei, X.; Zhang, F.; Song, T.; Sun, B. p-Type Doping Effect on the Performance of Organic-Inorganic Hybrid Solar Cells. *Appl. Phys. Lett.* **2011**, *99*, 233305.
- (4) Lüssem, B.; Riede, M.; Leo, K. Doping of Organic Semiconductors. *Phys. Status Solidi A* **2013**, *210*, 9.
- (5) Niu, X.; Qin, C.; Zhang, B.; Yang, J.; Xie, Z.; Cheng, Y.; Wang, L. Efficient Multilayer White Polymer Light-Emitting Diodes with Aluminum Cathodes. *Appl. Phys. Lett.* **2007**, *90*, 203513.
- (6) Sax, S.; Rugen-Penkalla, N.; Neuhold, A.; Schuh, S.; Zojer, E.; List, E. J. W.; Müllen, K. Efficient Blue-Light-Emitting Polymer Heterostructure Devices: The Fabrication of Multilayer Structures from Orthogonal Solvents. *Adv. Mater.* **2010**, *22*, 2087.
- (7) Aizawa, N.; Pu, Y. J.; Watanabe, M.; Chiba, T.; Ideta, K.; Toyota, N.; Igarashi, M.; Suzuri, Y.; Sasabe, H.; Kido, J. Solution-Processed Multilayer Small-Molecule Light-Emitting Devices with High-Efficiency White-Light Emission. *Nat. Commun.* **2014**, *5*, 5756.
- (8) Dai, A.; Zhou, Y.; Shu, A. L.; Mohapatra, S. K.; Wang, H.; Fuentes-Hernandez, C.; Zhang, Y.; Barlow, S.; Loo, Y. L.; Marder, S. R.; Kippelen, B.; Kahn, A. Enhanced Charge-Carrier Injection and Collection via Lamination of Doped Polymer Layers p-Doped with a Solution-Processible Molybdenum Complex. *Adv. Funct. Mater.* **2014**, *24*, 2197.
- (9) Kim, M. J.; Lee, M.; Min, H.; Kim, S.; Yang, J.; Kweon, H.; Lee, W.; Kim, D. H.; Choi, J.-H.; Ryu, D. Y.; Kang, M. S.; Kim, B. S.; Cho, J. H. Universal Three-Dimensional Crosslinker for All-Photopatterned Electronics. *Nat. Commun.* **2020**, *11*, 1520.
- (10) Zuniga, C. A.; Barlow, S.; Marder, S. R. Approaches to Solution-Processed Multilayer Organic Light-Emitting Diodes Based on Cross-Linking. *Chem. Mater.* **2011**, *23*, 658.
- (11) Zhang, Y. D.; Hreha, R. D.; Jabbar, G. E.; Kippelen, B.; Peyghambarian, N.; Marder, S. R. Photo-Crosslinkable Polymers as Hole-Transport Materials for Organic Light-Emitting Diodes. *J. Mater. Chem.* **2002**, *12*, 1703.
- (12) Cheng, Y. J.; Liu, M. S.; Zhang, Y.; Niu, Y.; Huang, F.; Ka, J. W.; Yip, Y.; Tian, A. K. Y.; Jen, A. K.-Y. Thermally Cross-Linkable Hole-Transporting Materials on Conducting Polymer: Synthesis, Characterization, and Applications for Polymer Light-Emitting Devices. *Chem. Mater.* **2008**, *20*, 413.
- (13) Dahlström, S.; Wilken, S.; Zhang, Y.; Ahläng, C.; Barlow, S.; Nyman, M.; Marder, S. R.; Österbacka, R. Cross-Linking of Doped Organic Semiconductor Interlayers for Organic Solar Cells: Potential and Challenges. *ACS Appl. Energy Mater.* **2021**, *4*, 14458.
- (14) Keana, J. F. W.; Xiong Cai, S. X. Functionalized Perfluorophenyl Azides: New Reagents for Photoaffinity Labeling. *J. Fluorine Chem.* **1989**, *43*, 151.
- (15) Poe, R.; Schnapp, K.; Young, M. J.; Grayzar, J.; Platz, M. S. Chemistry and Kinetics of Singlet (Pentafluorophenyl)Nitrene. *J. Am. Chem. Soc.* **1992**, *114*, 5054.
- (16) Park, J.; Lee, C.; Jung, J.; Kang, H.; Kim, K. H.; Ma, B.; Kim, B. J. Facile Photo-Crosslinking of Azide-Containing Hole-Transporting Polymers for Highly Efficient, Solution-Processed, Multilayer Organic Light Emitting Devices. *Adv. Funct. Mater.* **2014**, *24*, 7588.
- (17) Teo, D. W. Y.; Jamal, Z.; Phua, H. Y.; Tang, C. G.; Png, R. Q.; Chua, L. L. Nearly 100% Photocrosslinking Efficiency in Ultrahigh Work Function Hole-Doped Conjugated Polymers Using Bis-(Fluorophenyl Azide) Additives. *ACS Appl. Mater. Interfaces* **2019**, *11*, 48103.
- (18) Jacobs, I. E.; Li, J.; Burg, S. L.; Bilsky, D. J.; Rotondo, B. T.; Augustine, M. P.; Stroeve, P.; Moulé, A. J. Reversible Optical Control of Conjugated Polymer Solubility with Sub-Micrometer Resolution. *ACS Nano* **2015**, *9*, 1905.
- (19) Mansour, A. E.; Lungwitz, D.; Schultz, T.; Arvind, M.; Valencia, A. M.; Cocchi, C.; Opitz, A.; Neher, D.; Koch, N. The Optical Signatures of Molecular-Doping Induced Polarons in Poly(3-Hexylthiophene-2,5-diyl): Individual Polymer Chains: Versus Aggregates. *J. Mater. Chem. C* **2020**, *8*, 2870.
- (20) Duong, D. T.; Wang, C.; Antono, E.; Toney, M. F.; Salleo, A. The Chemical and Structural Origin of Efficient P-Type Doping in P3HT. *Org. Electron.* **2013**, *14*, 1330.
- (21) Cochran, J. E.; Junk, M. J. N.; Glauddell, A. M.; Miller, P. L.; Cowart, J. S.; Toney, M. F.; Hawker, C. J.; Chmelka, B. F.; Chabinc, M. L. Molecular Interactions and Ordering in Electrically Doped Polymers: Blends of PBTTT and F₄TCNQ. *Macromolecules* **2014**, *47*, 6836.
- (22) Zhang, Y.; de Boer, B.; Blom, P. W. M. Controllable Molecular Doping and Charge Transport in Solution-Processed Polymer Semiconducting Layers. *Adv. Funct. Mater.* **2009**, *19*, 1901.
- (23) Saeedifard, F.; Lungwitz, D.; Yu, Z.-D.; Schneider, S.; Mansour, A. E.; Opitz, A.; Barlow, S.; Toney, M. F.; Pei, J.; Koch, N.; Marder, S. R. Use of a Multiple Hydride Donor To Achieve an n-Doped Polymer with High Solvent Resistance. *ACS Appl. Mater. Interfaces* **2022**, *14*, 33598.
- (24) Tang, B.; Wu, Y.; Tai, A.; Hu, R.; Zhao, Z.; Shenqing, F. Z. Polytriazole with intrinsic flame retardance and preparing method and application thereof. Chinese Patent, CN 105906807 A, 2016.
- (25) Clark, J.; Silva, C.; Friend, R. H.; Spano, F. C. Role of Intermolecular Coupling in the Photophysics of Disordered Organic Semiconductors: Aggregate Emission in Regioregular Polythiophene. *Phys. Rev. Lett.* **2007**, *98*, 206406.
- (26) Brown, P. J.; Thomas, D. S.; Köhler, A.; Wilson, J. S.; Kim, J.-S.; Ramsdale, C. M.; Sirringhaus, H.; Friend, R. H. Effect of Interchain Interactions on the Absorption and Emission of Poly(3-Hexylthiophene). *Phys. Rev. B: Condens. Matter Mater. Phys.* **2003**, *67*, 064203.
- (27) Pingel, P.; Neher, D. Comprehensive Picture of p-Type Doping of P3HT with the Molecular Acceptor F₄TCNQ. *Phys. Rev. B: Condens. Matter Mater. Phys.* **2013**, *87*, 115209.
- (28) Müller, L.; Nanova, D.; Glaser, T.; Beck, S.; Pucci, A.; Kast, A. K.; Schröder, R. R.; Mankel, E.; Pingel, P.; Neher, D.; Kowalsky, W.; Lovrincic, R. Charge-Transfer-Solvent Interaction Predefines Doping Efficiency in p-Doped P3HT Films. *Chem. Mater.* **2016**, *28*, 4432.
- (29) Wegner, B.; Lungwitz, D.; Mansour, A. E.; Tait, C. E.; Tanaka, N.; Zhai, T.; Duhm, S.; Forster, M.; Behrends, J.; Shoji, Y.; Opitz, A.; Scherf, U.; List-Kratochvil, E. J. W.; Fukushima, T.; Koch, N. An Organic Borate Salt with Superior p-Doping Capability for Organic Semiconductors. *Adv. Sci.* **2020**, *7*, 2001322.
- (30) Köhler, A.; Bässler, H. *Electronic Processes in Organic Semiconductors: An Introduction*; WILEY-VCH Verlag GmbH & Co. KGaA: Weinheim, 2015.
- (31) Hu, H.; Zhao, K.; Fernandes, N.; Boufflet, P.; Bannock, J. H.; Yu, L.; de Mello, J. C.; Heeney, N.; Giannelis, M.; Amassian, E. P.; Amassian, A. Entanglements in Marginal Solutions: A Means of Tuning Pre-Aggregation of Conjugated Polymers with Positive Implications for Charge Transport. *J. Mater. Chem. C* **2015**, *3*, 7394.
- (32) Zhao, K.; Xue, L.; Liu, J.; Gao, X.; Wu, S.; Han, Y.; Geng, Y. A New Method to Improve Poly(3-Hexyl Thiophene) (P3HT) Crystalline Behavior: Decreasing Chains Entanglement to Promote Order-Disorder Transformation in Solution. *Langmuir* **2010**, *26*, 471.
- (33) Fried, J. R. *Polymer Science & Technology*, 3rd ed.; Prentice Hall: United States, 2014.
- (34) Noriega, R.; Rivnay, J.; Vandewal, K.; Koch, F. P. V.; Stingelin, N.; Smith, P.; Toney, M. F.; Salleo, A. A General Relationship between Disorder, Aggregation and Charge Transport in Conjugated Polymers. *Nat. Mater.* **2013**, *12*, 1038.
- (35) Yi, H. L.; Wu, C. H.; Wang, C. I.; Hua, C. C. Solvent-Regulated Mesoscale Aggregation Properties of Dilute PBTTT-C14 Solutions. *Macromolecules* **2017**, *50*, 5498.
- (36) Jacobs, I. E.; Aasen, E. W.; Oliveira, J. L.; Fonseca, T. N.; Roehling, J. D.; Li, J.; Zhang, G.; Augustine, M. P.; Mascal, M.; Moulé, A. J. Comparison of Solution-Mixed and Sequentially

Processed P3HT:F₄TCNQ Films: Effect of Doping-Induced Aggregation on Film Morphology. *J. Mater. Chem. C* **2016**, *4*, 3454.

(37) Mohapatra, S. K.; Zhang, Y.; Sandhu, B.; Fonari, M. S.; Timofeeva, T.; Marder, S. R.; Barlow, S. Synthesis Characterization, and Crystal Structures of Molybdenum Complexes of Unsymmetrical Electron-Poor Dithiolenes. *Polyhedron* **2016**, *116*, 88.

(38) Wegner, B.; Grubert, L.; Dennis, C.; Opitz, A.; Röttger, A.; Zhang, Y.; Barlow, S.; Marder, S. R.; Hecht, S.; Müllen, K.; Koch, N. Predicting the Yield of Ion Pair Formation in Molecular Electrical Doping: Redox-Potentials versus Ionization Energy/Electron Affinity. *J. Mater. Chem. C* **2019**, *7*, 13839.

(39) Gao, J.; Roehling, J. D.; Li, Y.; Guo, H.; Moulé, A. J.; Grey, J. K. The Effect of 2,3,5,6-Tetrafluoro-7,7,8,8-Tetracyanoquinodimethane Charge Transfer Dopants on the Conformation and Aggregation of Poly(3-Hexylthiophene). *J. Mater. Chem. C* **2013**, *1*, 5638.

(40) Street, R. A.; Northrup, J. E.; Salleo, A. Transport in Polycrystalline Polymer Thin-Film Transistors. *Phys. Rev. B: Condens. Matter Mater. Phys.* **2005**, *71*, 165202.

(41) Ko, S.; Hoke, E. T.; Pandey, L.; Hong, S.; Mondal, R.; Risko, C.; Yi, Y.; Noriega, R.; McGehee, M. D.; Brédas, J. L.; Salleo, A.; Bao, Z. Controlled Conjugated Backbone Twisting for an Increased Open-Circuit Voltage While Having a High Short-Circuit Current in Poly(Hexylthiophene) Derivatives. *J. Am. Chem. Soc.* **2012**, *134*, 5222.

(42) Cardona, C. M.; Li, W.; Kaifer, A. E.; Stockdale, D.; Bazan, G. C. Electrochemical Considerations for Determining Absolute Frontier Orbital Energy Levels of Conjugated Polymers for Solar Cell Applications. *Adv. Mater.* **2011**, *23*, 2367.

(43) Liang, Z.; Zhang, Y.; Souri, M.; Luo, X.; Boehm, A. M.; Li, R.; Zhang, Y.; Wang, T.; Kim, D. Y.; Mei, J.; Marder, S. R.; Graham, K. R. Influence of Dopant Size and Electron Affinity on the Electrical Conductivity and Thermoelectric Properties of a Series of Conjugated Polymers. *J. Mater. Chem. A* **2018**, *6*, 16495.

(44) Arvind, M.; Tait, C. E.; Guerrini, M.; Krumland, J.; Valencia, A. M.; Cocchi, C.; Mansour, A. E.; Koch, N.; Barlow, S.; Marder, S. R.; Behrends, J.; Neher, D. Quantitative Analysis of Doping-Induced Polarons and Charge-Transfer Complexes of Poly(3-Hexylthiophene) in Solution. *J. Phys. Chem. B* **2020**, *124*, 7694.

(45) Zhong, Y.; Untilova, V.; Muller, D.; Guchait, S.; Kiefer, C.; Herrmann, L.; Zimmermann, N.; Brosset, M.; Heiser, T.; Brinkmann, M. Preferential Location of Dopants in the Amorphous Phase of Oriented Regioregular Poly(3-Hexylthiophene-2,5-Diyl) Films Helps Reach Charge Conductivities of 3000 S Cm⁻¹. *Adv. Funct. Mater.* **2022**, *32*, 2202075.

(46) Lungwitz, D.; Schultz, T.; Tait, C. E.; Behrends, J.; Mohapatra, S. K.; Barlow, S.; Marder, S. R.; Opitz, A.; Koch, N. Disentangling Bulk and Interface Phenomena in a Molecularly Doped Polymer Semiconductor. *Adv. Opt. Mater.* **2021**, *9*, 2002039.

(47) Urquhart, S. G.; Martinson, M.; Eger, S.; Murcia, V.; Ade, H.; Collins, B. A. Connecting Molecular Conformation to Aggregation in P3HT Using near Edge X-Ray Absorption Fine Structure Spectroscopy. *J. Phys. Chem. C* **2017**, *121*, 21720.

(48) Lienhard, P. Caractérisation et Modélisation Du Vieillessement Des Photodiodes Organiques. Ph.D. Thesis, Université Grenoble Alpes, 2016.

Recommended by ACS

Highly Conductive Ultrathin Layers of Conjugated Polymers for Metal-Free Coplanar Transistors with Single-Polymer Transport Layers

Zichao Shen, Guanghao Lu, *et al.*

FEBRUARY 21, 2023

ACS APPLIED MATERIALS & INTERFACES

READ 

Adhesive Properties of Semiconducting Polymers: Poly(3-alkylthiophene) as an Ersatz Glue

Alexander X. Chen, Darren J. Lipomi, *et al.*

APRIL 04, 2023

CHEMISTRY OF MATERIALS

READ 

Chemical Vapor Deposition and High-Resolution Patterning of a Highly Conductive Two-Dimensional Coordination Polymer Film

Víctor Rubio-Giménez, Rob Ameloot, *et al.*

DECEMBER 19, 2022

JOURNAL OF THE AMERICAN CHEMICAL SOCIETY

READ 

Sequential-Twice-Doping Approach toward Synergistic Optimization of Carrier Concentration and Mobility in Thiophene-Based Polymers

Haoyu Chai, Lidong Chen, *et al.*

SEPTEMBER 22, 2022

ACS APPLIED ELECTRONIC MATERIALS

READ 

Get More Suggestions >